Effective absorption enhancement in small molecule organic solar cells using trapezoid gratings*

Xiang Chun-Ping(相春平)[a], Jin Yu(金 玉)[b], Liu Jie-Tao(刘杰涛)[a], Xu Bin-Zong(许斌宗)[a], Wang Wei-Min(汪卫敏)[a], Wei Xin(韦 欣)[a], Song Guo-Feng(宋国峰)[a], and Xu Yun(徐 云)[a]†

[a] *Nano-optoelectronics Laboratory, Institute of Semiconductors, Chinese Academy of Sciences, Beijing* 100083, *China*
[b] *College of Information Science and Engineering, Huaqiao University, Xiamen* 361021, *China*

(Received 13 May 2013; revised manuscript received 19 July 2013; published online 24 January 2014)

We demonstrate that the optical absorption is enhanced in small molecule organic solar cells by using a trapezoid grating structure. The enhanced absorption is mainly attributed to both waveguide modes and surface plasmon modes, which is simulated by using finite-difference time-domain method. The simulated results show that the surface plasmon along the semitransparent metallic Ag anode is excited by introducing the periodical trapezoid gratings, which induce the increase of high intensity field in the donor layer. Meanwhile, the waveguide modes result in a high intensity field in acceptor layer. The increase of field improves the absorption of organic solar cells significantly, which is demonstrated by simulating the electrical properties. The simulated results also show that the short-circuit current is increased by 31% in an optimized device, which is supported by the experimental measurement. Experimental result shows that the power conversion efficiency of the grating sample is increased by 7.7%.

Keywords: organic solar cells, localized surface plasmon, waveguide

PACS: 88.40.jr, 88.40.hj, 42.15.Eq, 42.79.DJ **DOI:** 10.1088/1674-1056/23/3/038803

1. Introduction

Organic solar cells (OSCs) have been of great interest in recent years for their unique properties of low-cost processing, mechanical flexibilities, and scalabilities, though their power conversion efficiency values are lower than those of the traditional silicon-based solar cells.[1,2] Up to now, the reported efficiency values of OSCs can reach 9.2% by using a tandem structure with different kinds of polymer materials,[3] and the efficiency values of small molecule organic solar cells (SMOSCs) are up to 12%.[4] However, the primary bottleneck of OSC is the trade-off between exciton diffusion and light absorption.[5,6] The optical absorption length of organic material is around 100 nm, while the exciton diffusion length is of the order of 10–50 nm.[7–10] Therefore, the absorption efficiency and exciton diffusion efficiency in a conventional OSC are coupled, opposing quantities; increasing absorption by increasing the device thickness leads to a decrease in exciton diffusion efficiency and vice versa.[11] Additionally, due to the mismatch of the work function between organic material and metal electrode, the charge collection efficiency of OSC is poor, which further limits the efficiency.[12] Hence, how to resolve these problems becomes a premise condition.

Recently, many approaches have been proposed to release this trade-off of OSCs. Among them, applying a metallic subwavelength structure in an OSC is a promising way to trap the incident light into organic layers.[6,8,13–20] The main effect of the subwavelength structure is that it can support the surface plasmon polaritons (SPPs) propagating along the metal/dielectric interface and the localized surface plasmon (LSP).[5,7,19,21,22] For small metallic nanoparticles with dimensions much smaller than the wavelength, the scattering efficiency is lower than the absorption efficiency, which results in obvious thermal loss.[13,23] In contrast to metallic nanoparticles, a periodical metallic nanograting with a tunable period can modulate the surface plasmon resonances and scatter photons into the active layer.[8] In previous work, a metallic nanograting has been used in a traditional silicon-based solar cell to improve the light harvest efficiency, which has been demonstrated by theoretical analysis.[11,17] In the present paper, we propose a process-compatible trapezoid nanograting structure in a top-illuminated SMOSC to increase the optical absorption efficiency. We optimize the grating structure by calculating the absorption spectra of the active layer, and reveal the reason for the absorption enhancement in different cases by analyzing the physical mechanisms. The simulated current density–voltage properties of the optimized device exhibits a significant improvement in optical absorption efficiency, which is further supported by experiment.

*Project supported by the National Natural Science Foundation of China (Grant Nos. 61036010 and 61177070), the National Basic Research Program of China (Grant Nos. 2011CBA00608 and 2012CB619203), and the National Key Research Program of China (Grant No. 2011ZX01015-001).

†Corresponding author. E-mail: xuyun@semi.ac.cn

© 2014 Chinese Physical Society and IOP Publishing Ltd

2. Model, calculation and experiment

2.1. Model and optical properties

We investigate the effect of a trapezoid nanograting in a top-illuminated SMOSC. The model is calculated by using the two-dimensional (2D) finite-difference time-domain (FDTD) method under the irradiations of transverse magnetic (TM) and transverse electric (TE) polarized light, separately. In our simulation, the grid size is set to be 2 nm×2 nm and the perfectly matched layer and the periodic boundary condition are used in the z direction and the x direction, respectively. The schematic diagram of the SMOSC is shown in Fig. 1. The silver (Ag) with nanograting structure is adopted as a substrate. Biphasic calcium phosphate (BCP) is introduced as an exciton blocking layer on the top of the cathode, and the fullerene (C_{60}) and subphthalocyanine (Subpc) are used as an accepter and a donor, respectively. A 20-nm-thick Ag anode is deposited on the top of the Subpc layer and presents a semitransparent property. The complex refractive indices of Subpc and BCP used for simulation are measured by spectroscopic ellipsometer and those of C_{60} and Ag are cited from Refs. [24] and [25].

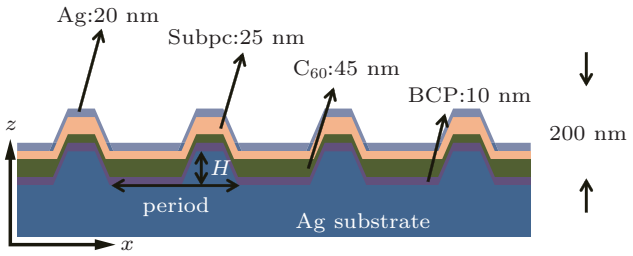


Fig. 1. (color online) Schematic diagram of the trapezoid grating top-illuminated SMOSC.

We first investigate the optical absorption properties of the proposed model. In order to characterize the absorption efficiency of the SMOSC, we particularly calculate the absorption of the active layer instead of the whole device. Figure 2(a) shows the values of the absorption coefficient α of Subpc and C_{60}, which is defined as $\alpha = 2\kappa(\omega)\omega/c$.[23] Here, κ is the extinction coefficient, ω is the angular frequency of the incidence, and c is the velocity of light in free space. Two separated intrinsic absorption regions corresponding to the donor and accepter give a broadband absorption spectrum of active layer, which, on the other hand, needs to be synthesized to obtain a maximum enhancement. We set the duty ratios of the grating to be 0.5 and 0.33 at the bottom and top side of the trapezoid respectively, while the grating height and period are considered to be optimized. Since the grating height is a main parameter which influences the scattering effect,[26] we first simulate the unpolarized optical absorption spectra of organic layers with grating heights from 0 nm to 125 nm (Fig. 2(b)), where the period is set to be 300 nm. The absorption spectrum is enhanced significantly from 350 nm to 620 nm, which are corresponding to the intrinsic absorptions of C_{60} and Subpc. The spectrum reaches a maximum value when the grating height reaches 100 nm, moreover, a larger grating height may reduce the optical absorption and electrical properties of the device.[17] To further understand the reason for the enhancement, the TE and TM polarized optical absorption spectra are calculated.

As shown in Fig. 2(c), the TE polarized optical absorption efficiency values of OSCs with a trapezoid nanograting structure are above 50% at wavelengths below 600 nm when the grating period is around 300 nm, which is higher than those of the planar OSCs with the same volume of active layer. The main reason for the TE polarized light absorption enhancement is the excitations of waveguide modes. By scattering the incident light into the active layer, the grating structure fulfills the phase matching condition of waveguide modes and increases the interaction of light with organic materials.[17] For normal incidence, the diffraction angle of the grating structure could be expressed as

$$n_{\text{org}}\Lambda\cos(\psi) = m\lambda, \tag{1}$$

where n_{org} is the refractive index of active layer, Λ is the period of the grating, ψ is the diffraction angle, m is the diffraction order, and λ is the free space wavelength. The phase matching condition of the waveguide modes resonance is

$$2k_{\text{org}}h - \varphi_1 - \varphi_2 = 2M\pi, \tag{2}$$

where the $k_{\text{org}} = 2n_{\text{org}}\pi\sin(\psi)/\lambda$ is the normal component of the propagating wave vector, h is the thickness of the waveguide layer, φ_1 and φ_2 are the polarization-depending phase shifts introduced by total internal reflection at the top and bottom surfaces of the waveguide respectively, and M is the mode order of the waveguide. As indicated from Eqs. (1) and (2), the resonant wavelength is red-shifted with the increase of period. To further elucidate the waveguide modes in organic layers, the distributions of electric field are shown in Fig. 3. Due to the fact that the refractive indices of C_{60} are higher than those of Subpc at wavelengths below 550 nm, the electric field is mainly localized in the C_{60} layer at the resonant wavelength (Fig. 3(a)). Moreover, when the wavelength of incident light is smaller than the resonant wavelength, the electric field is hard to couple into the waveguide layer (Fig. 3(b)). Consequently, an absorption valley is present in the range smaller than the resonance wavelength, and extends toward long wavelengths with the increase of period (Fig. 2(c)). Since the phase shifts φ_1 and φ_2 of the waveguide modes in TM polarization are larger than those in TE polarization,[26] the valley in the TM polarized absorption spectra appears at a shorter wavelength (Fig. 2(d)).

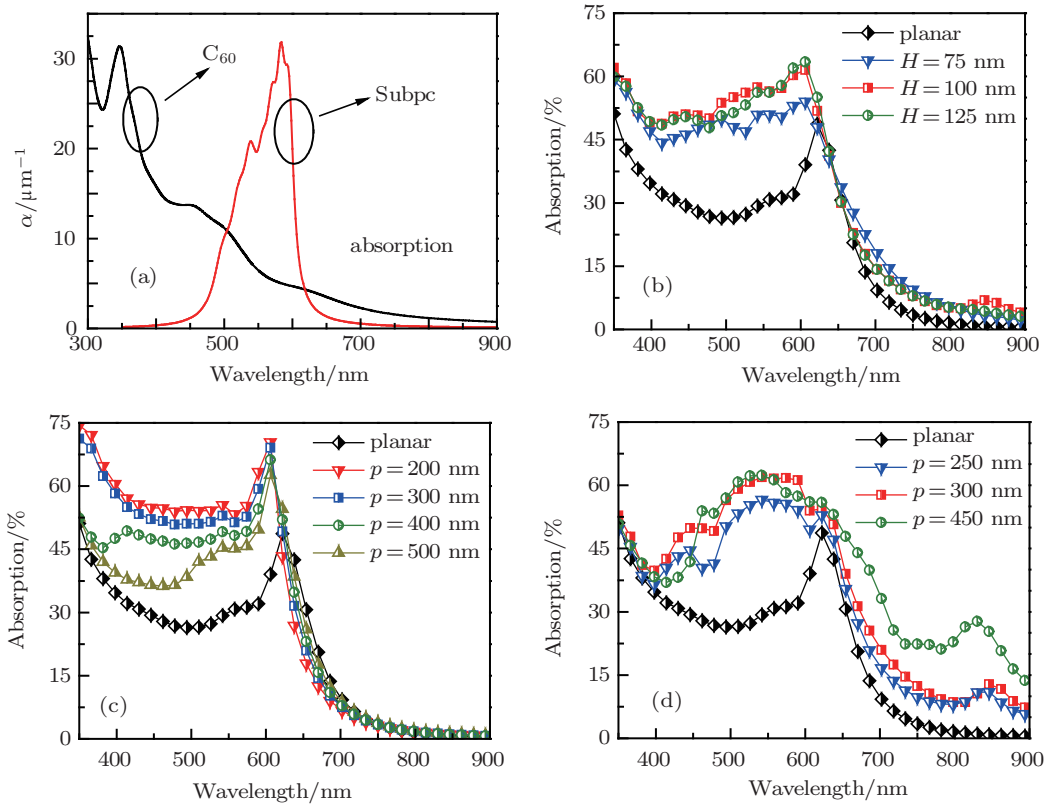


Fig. 2. (color online) (a) Absorption coefficient values of C_{60} and Subpc. (b) Unpolarized optical absorption spectra of the samples with different grating heights. (c) TE polarized absorption spectra of the samples with different grating periods. (d) Absorption spectra of the samples with different grating periods for TM polarization.

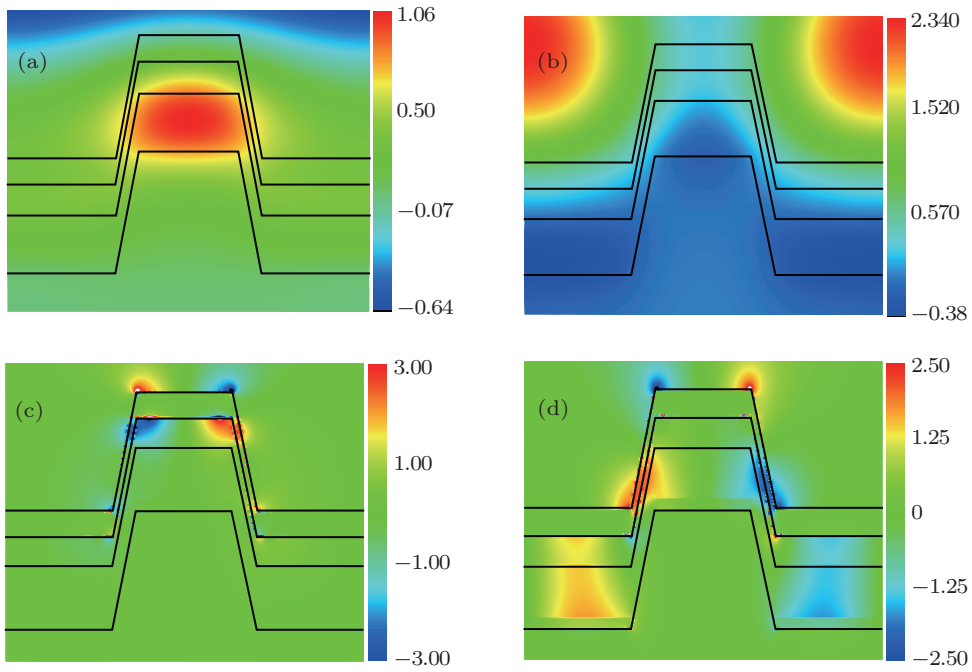


Fig. 3. (color online) Distributions of electric field at a wavelength of 400 nm with the period $\Lambda = 250$ nm (a) and at a wavelength of 420 nm with the period $\Lambda = 450$ nm (b), all under the irradiation of TE polarized light. The distributions of electric field at a wavelength of 455 nm with the period $\Lambda = 300$ nm (c), and at a wavelength of 830 nm with the period $\Lambda = 450$ nm (d), all under the irradiation of TM polarized light.

Not only can the waveguide modes be excited by the TM polarized light and increase the TM polarized absorption, but also the SPPs and LSP.[23] In the case of a small period (under 300 nm), the LSP is the main reason for TM polarized absorption enhancement.[7] The LSP resonance can be excited directly by the incident light and the interaction of LSP at each unit cell comes into effect as the period decreases.[23] As the grating vector is perpendicular to the wave vector, the

longitudinal LSP mode can be excited by the normal incident light around $\lambda = 450$ nm and performs a red-shift with the increase of period. The electric field is localized at the place close to the anode at the top of the trapezoid grating at the longitudinal LSP resonance, which can increase the absorption of Subpc obviously (Fig. 3(c)). Due to the non-uniform dimension of the trapezoid with a narrow top and wide bottom in each unit cell, a broadband absorption enhancement corresponding to the absorption of Subpc (at wavelength 500 nm −600 nm) exhibits an absorption efficiency of above 60%, which is twice higher than that of the planar device. This increment arises from the excitation of LSP modes with the energy mostly localized on the bevel of the trapezoid, which could signally increase the current density since the active layer of the resonant region is thin for exciton diffusion.[17] As the grating period increases, the SPPs come into effect at long wavelengths,[7] with the electric field mostly confined at the bottom of the grating (Fig. 3(d)). The absorption of the device with period $\Lambda = 450$ nm exhibits an absorption enhancement at $\lambda = 830$ nm compared with that of the device of which the period is smaller.

2.2. Current density–voltage characteristics of the proposed device

To demonstrate the electrical performances of the proposed thin-film SMOSCs devices, we calculate the current density–voltage curves of the device under unpolarized AM 1.5G illumination. In our simulation, we assume that each photon generates one electric–hole pair. As the band gap of C_{60} is about 1.9 eV[24] and the intrinsic absorption region of Subpc is from 450 nm to 650 nm, the photon with energy lower than 1.9 eV is hard to excite the exciton and transforms into heat ultimately. Thus, we particularly consider the absorption spectrum between 350 nm and 700 nm. As shown in Fig. 4, the short-circuit current density of the device with grating period $\Lambda = 300$ nm increases to 7.37 mA/cm^2, 31% higher than that of the planar device (5.62 mA/cm^2). The device with period $\Lambda = 450$ nm shows a relatively low current density since the waveguide modes cannot couple into the C_{60} layer in the intrinsic absorption region.

In order to confirm the simulation results, we fabricate devices each with an area of 2 mm×2 mm on the grating substrate. We firstly fabricate a one-dimensional (1D) nanograting by using interference lithography. A laser beam at $\lambda = 325$ nm is used to generate the interference pattern on a 100 nm-thick photoresist layer, followed by developing. The substrate is etched by inductively coupled plasma (ICP) etching technology to form trapezoid gratings, and the scanning electron microscope (SEM) image of the grating structure is shown in Fig. 5(a). Afterward Ag (100 nm)/Ca (1 nm)/BCP (10 nm)/C_{60} (45 nm)/Subpc (25 nm)/Ag (20 nm) are fabricated by a vacuum thermal evaporation process sequentially and the thickness of each layer is monitored by a quartz crystal film thickness monitor. The ultrathin Ca modified layer is deposited to form an ohmic contact, which can reduce the contact resistance without influencing the optical properties of the device. In order to demonstrate the enhancement effect, the OSC device with a planar structure is also fabricated as a reference sample. The current density–voltage characteristic curves of the device are measured under 100 mW/cm^2 AM 1.5G illumination (Fig. 5(b)). By increasing the optical absorption (or alternatively, the generation rate of excitons) of the device, the short-circuit current density of the sample with the grating structure increases to 3.93 mA/cm^2, 16.4% higher than that of the planar device which is 3.38 mA/cm^2. The power conversion efficiency exhibits an enhancement of 7.7% (increases from 1.51% to 1.63%). Meanwhile, the filling factor (FF) of the grating sample (39.8%) shows a negligible decrement compared with the planar one (41.4%), indicating an acceptable processing compatibility of the trapezoid grating SMOSC.

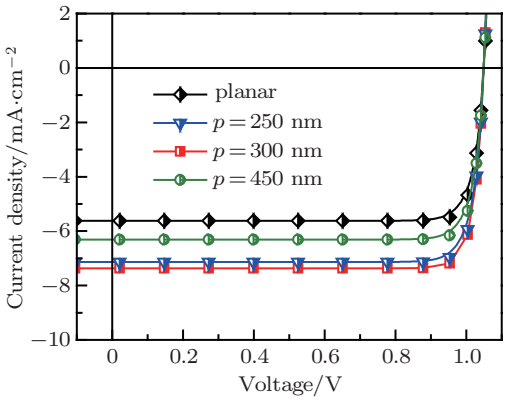


Fig. 4. (color online) Simulated current density–voltage curves of the system for different periods.

Compared with the experimental results, the simulated current density is high because the photovoltaic properties of organic materials and the mismatch of the work function of different materials (i.e., the internal quantum efficiency and the charge collection efficiency) are not taken into account in our simulation. Moreover, the larger interface area of the grating sample increases the surface recombination hence leads to a low charge collection efficiency compared with that of the planar sample, which results in a decreased increment of short-circuit current density (from 31% to 16.4%).[17,27] The FF of the device, the major difference between the simulation (about 88%) and experiment (about 40%), is mainly caused by the unavoidable leakage current and series resistance. The Ca modified layer can reduce the series resistance and suppress

the decrease of FF. Nevertheless, the reduction in the open-circuit voltage of the grating sample (Fig. 5(b)) indicates that the leakage current, which increases with the increase of interface area and the decrease of shunt resistance, is the main reason for the decrease of FF.[27] It is noted that the understanding of the physical mechanism could open up a new way to engineer and optimize other structures by this method. Moreover, a 2D grating structure can be processed to realize a further improved light-trapping effect.

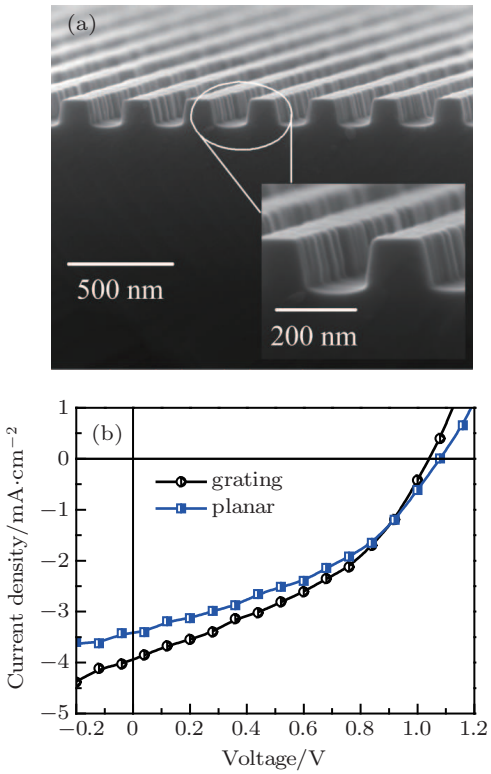


Fig. 5. (color online) (a) SEM cross-sectional view of the grating. The grating height is 110 nm and the period is 300 nm. (b) Measured current density-voltage curves for the device with a grating period of 300 nm.

3. Conclusions

In the present paper, we investigate the effect of trapezoid grating on both TE and TM polarized optical absorptions of a top-illuminated SMOSC. A significant enhancement caused by waveguide and LSP modes below 600 nm is observed, and the SPPs are excited around 800 nm. We improve the intrinsic absorption of the active layer by adjusting the grating period and grating height. The simulated and experimental short-circuit current densities of the device with the grating structure are increased by 31% and 16.4% compared with the short-circuit current density of the planar device, respectively. The use of the trapezoid grating in top-illuminated SMOSCs improves the power conversion efficiency by 7.7% in experiment. The proposed design, simulation and fabrication can potentially be extended to different types of low-cost ultra-thin OSCs.

References

[1] Hoppe H and Sariciftci N S 2004 *J. Mater. Res.* **19** 1924
[2] Chopra K L, Paulson P D and Dutta V 2004 *Prog. Photovolt.* **12** 69
[3] He Z, Zhong C, Su S, Xu M, Wu H and Cao Y 2012 *Nat. Photonics* **6** 591
[4] Die Heliatek GmbH http://www.heliatek.com [2013]
[5] Atwater H A and Polman A 2010 *Nat. Mater.* **9** 205
[6] Williamson A, McClean E, Leipold D, Zerulla D and Runge E 2011 *Appl. Phys. Lett.* **99** 093307
[7] Shen H and Maes B 2011 *Opt. Express* **19** A1202
[8] Jin Y, Feng J, Zhang X L, Xu M, Bi Y G, Chen Q D, Wang H Y and Sun H B 2012 *Appl. Phys. Lett.* **101** 163303
[9] Liu X D, Xu Z, Zhang F J, Zhao S L, Zhang T H, Gong W, Song J L, Kong C, Yan G A and Xu X R 2010 *Chin. Phys. B* **19** 118601
[10] Peumans P, Uchida S and Forrest S R 2003 *Nature* **425** 158
[11] Pala R A, White J, Barnard E, Liu J and Brongersma M L 2009 *Adv. Mater.* **21** 3504
[12] Kim J Y, Lee K, Coates N E, Moses D, Nguyen T Q, Dante M and Heeger A J 2007 *Science* **317** 222
[13] Bai W L, Gan Q Q, Song G F, Chen L H, Kafafi Z and Bartoli F 2010 *Opt. Express* **18** A620
[14] Gao H L, Zhang X W, Yin Z G, Tan H R, Zhang S G, Meng J H and Liu X 2012 *Appl. Phys. Lett.* **101** 133903
[15] Tvingstedt K, Persson N K, Inganas O, Rahachou A and Zozoulenko I V 2007 *Appl. Phys. Lett.* **91** 113514
[16] Wang W, Wu S M, Reinhardt K, Lu Y L and Chen S C 2010 *Nano Lett.* **10** 2012
[17] Deceglie M G, Ferry V E, Alivisatos A P and Atwater H A 2012 *Nano Lett.* **12** 2894
[18] Tan H R, Santbergen R, Smets A H M and Zeman M 2012 *Nano Lett.* **12** 4070
[19] Li X H, Choy W C H, Huo L J, Xie F X, Sha W E I, Ding B F, Guo X, Li Y F, Hou J H, You J B and Yang Y 2012 *Adv. Mater.* **24** 3046
[20] Heng G G, Jiang J L, Xian F L, Qiang H X, Wu H and Li X Y 2011 *Chin. Phys. B* **20** 094201
[21] Yang M, Fu Z P, Lin F and Zhu X 2011 *Opt. Express* **19** A763
[22] Dong L M and Xu H X 2012 *Physics* **41** 582 (in Chinese)
[23] Maier S A 2007 *Plasmonics: Fundamental and Applications* Vol. 1 (New York: Springer Science+ Business Media LLC) p. 10
[24] Kelly M K, Etchegoin P, Fuchs D, Kratschmer W and Fostiropoulos K 1992 *Phys. Rev. B* **46** 4963
[25] Palik E D 1985 *Handbook of Optical Constants of Solids* Vol. 1 (Orlando, Florida: Harcourt Brace Jovanovich) p. 350
[26] Feng S F, Zhang X P, Song J Y, Liu H M and Song Y R 2009 *Opt. Express* **17** 426
[27] Yang X L and Deng J X 2012 *Physics* **41** 669 (in Chinese)